A sulphated glycosaminoglycan extract from *Placopecten magellanicus* inhibits the Alzheimer's disease β-Site amyloid precursor protein cleaving enzyme 1 (BACE-1).

Courtney J. Mycroft-West [1#*], Anthony J. Devlin [1, 2], Lynsay C. Cooper [3], Scott E. Guimond [1], Patricia Procter [1], Gavin J. Miller [1], Marco Guerrini [2], David G. Fernig [4], Edwin A. Yates [4], Marcelo A. Lima [1] and Mark A. Skidmore [1, 4*]

[1] Centre for Glycoscience Research, Keele University, Keele, Staffordshire, ST5 5BG, UK; courtney.mycroft-west@rfi.ac.uk (C.J.M.-W.); a.devlin1@keele.ac.uk (A.J.D.); s.e.guimond@keele.ac.uk (S.E.G); p.procter@keele.ac.uk (P.P.); g.j.miller@keele.ac.uk (G.J.M.); m.andrade.de.lima@keele.ac.uk (M.A.L.); m.a.skidmore@keele.ac.uk (M.A.S)

[2] Istituto di Ricerche Chimiche e Biochimiche G. Ronzoni, Via G. Colombo 81, 20133 Milan, Italy; a.devlin1@keele.ac.uk (A.J.D.); guerrini@ronzoni.it (M.G.)

[3] University of Gloucestershire, The Park, Cheltenham, GL50 2RH, UK; lcooper1@glos.ac.uk

[4] Department of Biochemistry and Systems Biology, ISMIB, University of Liverpool, Crown Street, Liverpool L69 7ZB, UK; dgfernig@liverpool.ac.uk (D.G.F); E.A.Yates@liverpool.ac.uk (E.A.Y); m.a.skidmore@keele.ac.uk (M.A.S)

* Corresponding authors: courtney.mycroft-west@rfi.ac.uk; (C.J.M.-W.); m.a.skidmore@keele.ac.uk; (M.A.S)

\# Current contact details: The Rosalind Franklin Institute, Harwell Campus, Didcot, OX11 0QX, UK; courtney.mycroft-west@rfi.ac.uk

Highlights:

- *A glycosaminoglycan extract from the Atlantic Sea Scallop, Placopecten magellanicus, displays high inhibitory potential for BACE-1, a key drug-target in Alzheimer's disease.*
- *The composition of the extract is predominantly that of heparan sulphate, containing a high content of the disaccharide UA-GlcNAc(6S), which is uncommon in mammalian-derived HS samples.*
- *The glycosaminoglycan extract possesses highly attenuated anticoagulant potential compared to mammalian heparin.*

Abstract: The clinically important anticoagulant heparin, a member of the glycosaminoglycan family of carbohydrates that is extracted predominantly from porcine and bovine tissue sources, has previously been shown to inhibit the β-Site amyloid precursor protein cleaving enzyme 1 (BACE-1), a key drug target in Alzheimer's Disease. In addition, heparin has been shown to exert favourable bioactivities through a number of pathophysiological pathways involved in the disease processes of Alzheimer's Disease including inflammation, oxidative stress, tau phosphorylation and amyloid peptide generation. Despite the multi-target potential of heparin as a therapeutic option for Alzheimer's disease, the repurposing of this medically important biomolecule has to-date been precluded by its high anticoagulant potential. An alternative source to mammalian-derived glycosaminoglycans are those extracted from marine environments and these have been shown to display an expanded repertoire of sequence-space and heterogeneity compared to their mammalian counterparts. Furthermore, many marine-derived glycosaminoglycans appear to retain favourable bioactivities, whilst lacking the high anticoagulant potential of their mammalian counterparts. Here we describe a sulphated, marine-derived glycosaminoglycan extract from the Atlantic Sea Scallop, *Placopecten magellanicus* that displays high inhibitory potential against BACE-1 (IC_{50} = 4.8 $\mu g.mL^{-1}$) combined with low anticoagulant activity; 25-fold less than that of heparin. This extract possesses a more favourable therapeutic profile compared to pharmaceutical heparin of mammalian provenance and is composed of a mixture of heparan sulphate (HS), with a high content of 6-sulphated N-acetyl glucosamine (64 %), and chondroitin sulphate.

Keywords: Alzheimer's disease; amyloid-β; BACE-1; β-secretase; β-Site amyloid precursor protein cleaving enzyme 1; glycosaminoglycan; chondroitin sulphate; heparin; heparan sulphate, *Placopecten magellanicus.*

1. Introduction

Glycosaminoglycans (GAGs) are heterogeneous polysaccharides located extensively throughout almost all mammalian tissues, where they are found either intracellularly, tethered to the cell membrane, or secreted into the extracellular matrix [1]. There are four classes of GAG, including heparin/heparan sulphate (HS), chondroitin sulphate (CS)/ dermatan sulphate (DS), hyaluronic acid (HA) and keratan sulphate (KS). Each class of GAG comprises a distinctive underlying disaccharide repeat unit of a uronic acid residue (β-D-glucuronic acid; GlcA or the C5 epimer α-L-iduronic acid; IdoA) or in the case of KS, galactose, linked to either *N*-acetyl-β-D-galactosamine (GalNAc) or *N*-acetyl-β/α-D-glucosamine residue (GlcNAc). The repeating disaccharide units that comprise each GAG chain can undergo variable levels of sulphation, which occur at characteristic positions for each subtype of GAG; these modifications do not go to completion throughout the polysaccharide chain. Out of all the GAGs, the extent of possible modification is the most diverse for HS, where for each disaccharide there exists a theoretical total of 48 potential disaccharide structures. In addition, the length of GAGs can be extensive and variable, imparting further heterogeneity upon this class of polysaccharides [1–3]. Glycosaminoglycan chains, with the exception of HA, are synthesised attached to a protein core in the Golgi, of which over 40 have been identified and are together termed proteoglycans (PG). The identity of PG core protein is implicated in the identity and modification pattern of the subsequently attached GAG chains, further increasing complexity [4]. The high degree of structural variability and ubiquitous presence of GAGs affords this class of polysaccharides an extensive array of biological functions, examples of which are wide ranging, including structural scaffolds, immunological modulators and regulators of proliferation and differentiation. Proteoglycans, in particular those bearing HS chains, have also been widely implicated in amyloidogenic disease, for example Alzheimer's disease, where alterations in the fine structure of the polysaccharide chain are associated with pathology (for an extensive review, see [5].

One identified function of the glycosaminoglycan HS is that of a physiological regulator for the principal neuronal β-secretase, BACE-1 [6]. BACE-1 undertakes the rate-limiting cleavage of the amyloid precursor protein (APP), where further processing terminates with the production of Aβ peptides, which are suggested to be one of the causative agents of AD. In this amyloidogenic pathway of APP metabolism, APP is initially cleaved by BACE-1 to yield a membrane tethered C-terminal fragment (CTF-99) and a N-terminal soluble fragment (sAPPβ). Further proteolytic cleavage of CTF-99 by γ-secretase results in Aβ peptides of variable length, which can subsequently undergo fibrillization into neurotoxic aggregates [7,8]. Furthermore, the amyloidogenic hypothesis of AD regards Aβ as the initiating factor for other characteristic AD pathologies, such as neurofibrillary tangles (NFTs) and inflammation, which contribute to the extensive brain atrophy observed [9]. Inhibition of the enzymatic activity of BACE-1 would, therefore, result in reduced Aβ peptide production, thereby ameliorating downstream pathological events. As a result, BACE-1 has become an attractive target for the design of inhibitors as potential therapeutic agents for AD. Despite this, the design of synthetic peptide based BACE-1 inhibitors has been hampered by the large substrate binding cleft of the enzyme and the inability of inhibitors to cross the blood brain barrier (BBB) [10].

The pharmaceutical anticoagulant heparin, which is structurally related to HS, has been demonstrated to inhibit BACE-1 [6], while heparin oligosaccharides have been shown to cross the BBB [11] . Furthermore, in transgenic mouse models, low molecular weight heparin (LMWH) and porcine HS have been observed to enhance Aβ clearance through multiple mechanisms, which led to reduced Aβ deposition and improved cognitive functioning in mice [12–14]. Therefore, the utilisation of drugs based upon heparin or HS holds great promise as potential treatment options for AD, targeting the imbalance of Aβ production and clearance, which has been widely postulated to be the underlying aetiology of the disease. A major obstacle for the repurposing of pharmaceutical heparin, or LMWH derivatives, as pharmaceutical agents for the treatment of AD is the potent anticoagulant activity of this class of molecules. However, HS with altered sulphate modifications compared to heparin, e.g. glucosamine residues bearing NAc as opposed to NS, are known to display significantly attenuated anticoagulant activity [15]. The discovery of natural HS sources that exhibit greatly reduced anticoagulant activity, whilst retaining structural patterning that bestow favourable bioactivities, for instance BACE-1 inhibition, would be greatly beneficial to the discovery of future GAG-based therapeutics.

A potential source of natural GAGs for therapeutic applications is that of commonly farmed marine organisms. In contrast to GAGs sourced from mammals, marine species have been demonstrated to possess GAGs variable modification patterns that are unique [3,16–26]. The expanded structural diversity displayed by GAGs sourced from marine species can be utilised to probe for modifications that confer optimal therapeutic activities. Once identified, these sequences can be exploited for the development of saccharides with defined sequences by chemical or chemoenzymatic synthesis. Alternatively, utilisation of species that can be farmed using sustainable methods, for instance aquaculture, for the sourcing of GAGs for therapeutic applications could prove to be viable. Herein, the Atlantic sea scallop, *Placopecten magellanicus*, was used as a source organism for the extraction of GAGs, which were subsequently characterised, evaluated for their anticoagulant activity and the ability to inhibit BACE-1.

2. Results

2.1. Isolation of glycosaminoglycans from Placopecten magellanicus with BACE-1 inhibitory activity and reduced anticoagulant properties

Glycosaminoglycans from *P. magellanicus* were released from delipidated tissue via proteolysis and the free peptidoglycan chains were subsequently captured using strong anion exchange resin prior to elution with 2M NaCl. Glycosaminoglycans were precipitated from the eluate by methanol addition before being subjected to further purification using DEAE-anion exchange chromatography, in which a stepwise NaCl gradient was employed for elution. The DEAE eluate obtained at 1 M NaCl, designated as fraction 5 (F5), was observed to possess high BACE-1 inhibitory activity, as determined by the previously described FRET assay, which employs a quenched, fluorogenic peptide substrate based upon the APP_{SW} mutation (6,16–18; Figure 1B). The IC_{50} of BACE-1 inhibition by porcine heparin was in accordance with previous reports at ~ 2.5 $\mu g.mL^{-1}$, with maximum inhibition being achieved at 5 $\mu g.mL^{-1}$[6,16–18]. The F5 extract obtained from *P. magellanicus* was observed to possess BACE-1 inhibitory activity ~ two fold lower than that of porcine heparin, with an IC_{50} of 4.8 $\mu g.mL^{-1}$ and maximum inhibition at concentrations > 10 $\mu g.mL^{-1}$ (Figure 1B). At low concentrations of porcine heparin, and the *P. magellanicus* F5 extract, an increase in BACE-1 activity was observed; however, this effect was lower for the *P. magellanicus* F5 extract (Figure 1B). Both chondroitinase (ABC) and heparinase (I & III) treatment of the *P. magellanicus* F5 extract resulted in a product that retained ~ 50% BACE-1 activity of the undigested extract (S3). This would suggest that the BACE-1 inhibitory activity of the *P. magellanicus* F5 extract resides in both the glucosaminoglycans and galactosaminoglycans constituents present within the sample and cannot be attributed to either the heparan sulphate or chondroitin sulphate components exclusively.

A change in the melting temperature (ΔT_m) of BACE-1, measured by differential scanning fluorimetry (DSF), has previously been observed in the presence of GAGs and other BACE-1 inhibitors. The extent of the shift in T_m of BACE-1 has been employed as an indicative screen to evaluate the potency of potential BACE-1 inhibitors [16–18,27,28]. When screened using DSF, *P. magellanicus* F5 induced a Δ 8.8°C reduction in the T_m of BACE-1 at concentrations > 50 $\mu g.mL^{-1}$(Figure 1C; $\pm$, SD = 0.3, n= 3). This is marginally reduced in comparison to the ΔT_m of BACE-1 observed in the presence of porcine heparin at an equivalent concentration; ~ Δ9.6°C (Figure 1C; $\pm$, SD = 0.3, n= 3), which may be indicative of the marginally reduced potency of the *P. magellanicus* F5 extract. The observed negative shift in the T_m of BACE-1 in the presence of both *P. magellanicus* F5 and porcine heparin was also found to be dose-dependent with an EC_{50} of 7 $\mu g.mL^{-1}$ and 4 $\mu g.mL^{-1}$ respectively (Figure 1D).

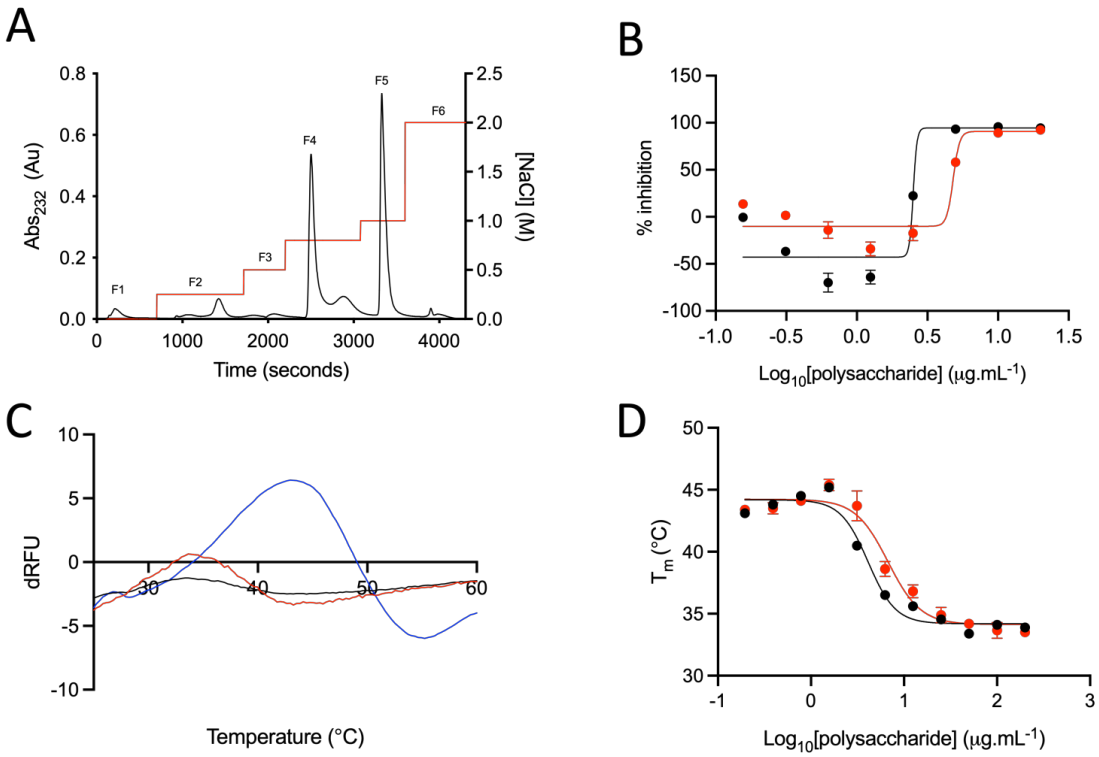

Figure 1. DEAE weak anion exchange chromatography of glycosaminoglycans obtained from *P. magellanicus*. Bound material was eluted with a stepwise NaCl gradient from 0 - 2 M NaCl (red; fractions F1 - F6), with in-line monitoring at 232 nm (black).* *P. magellanicus* F5 was taken forward for analysis due to this fraction possessing BACE-1 inhibitory activity; (B) BACE-1 inhibitory activity was determined by a quenched fluorogenic FRET peptide assay; *P. magellanicus* F5 (red) IC_{50} = 4.8 (R^2 = 0.91) μg.mL^{-1}, porcine heparin (black) IC_{50} = 2.5 μg.mL^{-1} (R^2 = 0.91), data represented as % inhibition $\pm$ SD (n=3). (C) First differential of the DSF thermal stability profile of BACE-1 with heparin (black), *P. magellanicus* F5 (red) or alone (blue) in 50 mM sodium acetate buffer pH 4.0. (D) T_m of BACE-1 with increasing heparin (black) or *P. magellanicus* F5 (red) concentration.

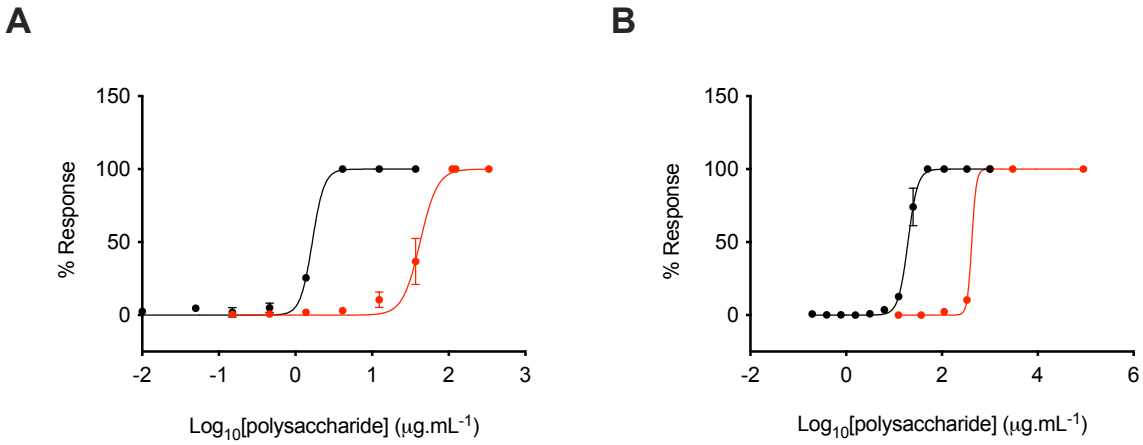

Figure 2: Anticoagulant activity of *P. magellanicus* F5. (A) Activated partial thromboplastin time (aPTT) represented as % inhibitory response ± SD, n=3. *P. magellanicus* F5 (red) and porcine heparin (black) EC_{50} = 42.3 μg.mL^{-1} and 1.7 μg.mL^{-1}, respectively. (B) prothrombin time (PT) represented as % inhibitory response ± SD, n=3. *P. magellanicus* F5 (red) and porcine heparin (black) EC_{50} = 419.8 μg.mL^{-1} and 19.3 μg.mL^{-1}, respectively.

As documented, the potent anticoagulant activity of heparin prevents the future repurposing of this clinically approved drug for alternative therapeutic applications, for example in AD [15]. Therefore, the anticoagulant activity of the *P. magellanicus* F5 extract was evaluated by comparing the anticoagulant response to that of porcine heparin (193 $IU.mg^{-1}$), in the activated partial thromboplastin time (aPTT; intrinsic pathway) and prothrombin time (PT; extrinsic pathway) assays. *P. magellanicus* F5 was observed to exhibit an approximate 25-fold reduction in activity to porcine heparin, when evaluated using the aPTT assay, at EC_{50} = 42.3 $\mu g.mL^{-1}$ and 1.70 $\mu g.mL^{-1}$, respectively. Similarly, in the PT assay the *P. magellanicus* F5 extract was observed to display a ~ 25-fold reduction in activity in comparison to porcine heparin; EC_{50} = 419.8 $\mu g.mL^{-1}$ and 19.30 $\mu g.mL^{-1}$, respectively (Figure 2). As a result, when considering the reduced anticoagulant activity of the P. *magellanicus* F5 extract, this compound represents a ~ 10-fold increase in therapeutic value over clinically approved, porcine unfractionated heparin (Table 1). Structural analysis of the *P. magellanicus* F5 extract was subsequently performed in order to establish the composition of the extract.

	BACE-1 inhibitory activity ($\mu g.mL^{-1}$)	**Anticoagulant activity ($\mu g.mL^{-1}$)**	**Therapeutic ratio**
P. magellanicus F5	4.8	42.3	8.8
Heparin	2.5	1.70	0.7

Table 1. Therapeutic value of *P. magellanicus* F5 and porcine heparin calculated using the ratio of the IC_{50}s of anticoagulant activity and BACE-1 inhibitory activity (measured by aPTT and FRET, respectively). aPTT = activated partial thromboplastin time, PT = prothrombin time.

2.2. Characterisation of the glycosaminoglycan extract from Placopecten magellanicus

The *P. magellanicus* F5 extract was confirmed to contain heparin/heparan sulphate and chondroitin/dermatan sulphate by agarose-gel electrophoresis and enzymatic digestion with *Pedobacter heparinus* heparinase lyases (Figure 3). A component with electrophoretic mobility corresponding to HS/heparin was observed, which was degraded when subjected to heparinase treatment (Figure 3B), indicating the presence of glucosaminoglycans within the *P. magellanicus* F5 extract. The *P. magellanicus* F5 sample also possessed a minor band migrating the same distance as the galactosaminoglycan-containing standards, this band was not degraded upon heparitinase treatment indicating the presence of chondroitin and/or dermatan sulphate within the sample.

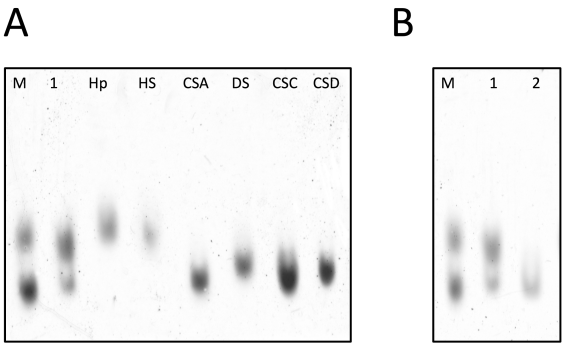

Figure 3. (A, B) Agarose gel electrophoresis of *P. magellanicus* F5 alone (1) or digested with *Pedobacter heparinus* heparinase lyases I, II and III (2) compared to glycosaminoglycan standards heparin (Hp) heparan sulphate (HS), dermatan sulphate (DS) and chondroitin sulphate A, C and D (CSA, CSC and CSD, respectively), M = mixture of CSA and heparin.

The ATR-FTIR spectra of the *P. magellanicus* F5 contains spectral features that are indicative of GAGs, e.g., the peaks present at 1230, 1430, 1635 cm^{-1} and 1559 cm^{-1}, which correspond to S=O, symmetric carbonyl stretching, asymmetric stretching carbonyl stretching, and coupled C-N vibrations of N-acetyl (amide) groups, respectively. The peaks present at 990 cm^{-1} and 1025 cm^{-1} have also been attributed to C-O-C glycosidic bond stretches [29–32] and can be used to differentiate between GAGs, such as CS and HS, due to disparities in the glycosidic linkages of these polysaccharides. For HS a band of higher intensity can be observed at 990 cm^{-1}, whereas for CS the prominent band is seen at 1025 cm^{-1}. The ATR-FTIR spectra of the *P. magellanicus* F5 extract contained a peak at both 990 cm^{-1} and 1025 cm^{-1}, again suggesting that the sample is composed of a mixture of CS/DS and HS/heparin.

Using principal component analysis (PCA) the attenuated total reflectance Fourier transform infrared (ATR-FTIR) spectra of *P. magellanicus* F5 extract was compared to that of a library of GAG standards; comprising 185 heparins, 31 HS, 44 CSs and dermatan sulphates (DS), 11 hyaluronic acid (HA) and 6 over sulphated chondroitin sulphates (OCSC). The complexity of the ATR-FTIR spectra of GAGs, which is a result of broad overlapping signals, renders spectral assignment challenging. Despite this, deconvolution of GAG ATR-FTIR spectra by PCA can successfully discriminate between GAG subclasses and has been shown to detect the presence of contaminants, for instance the presence of OSCS within pharmaceutical heparin preparations [29]. As a result, this approach was utilised to further evaluate the GAG composition of the *P. magellanicus* F5 extract, which was identified to contain a mixture of HS/heparin and galactosaminoglycans by agarose gel electrophoresis. Of note the region > 3000 cm^{-1} (OH stretch region), which is associated with variations in environmental moisture levels during sample acquisition, was discarded prior to PCA, as variations in this region are not likely to result from underlying structural differences between samples. Principal component 1, which covers 57% of the total variance, separated the *P. magellanicus* F5 extract alongside HS, CS and OSCS standards. However, when PC1 and PC2 were compared (covering 72% of the total variance), the *P. magellanicus* F5 extract was further separated towards the region containing CS standards (Figure 4).

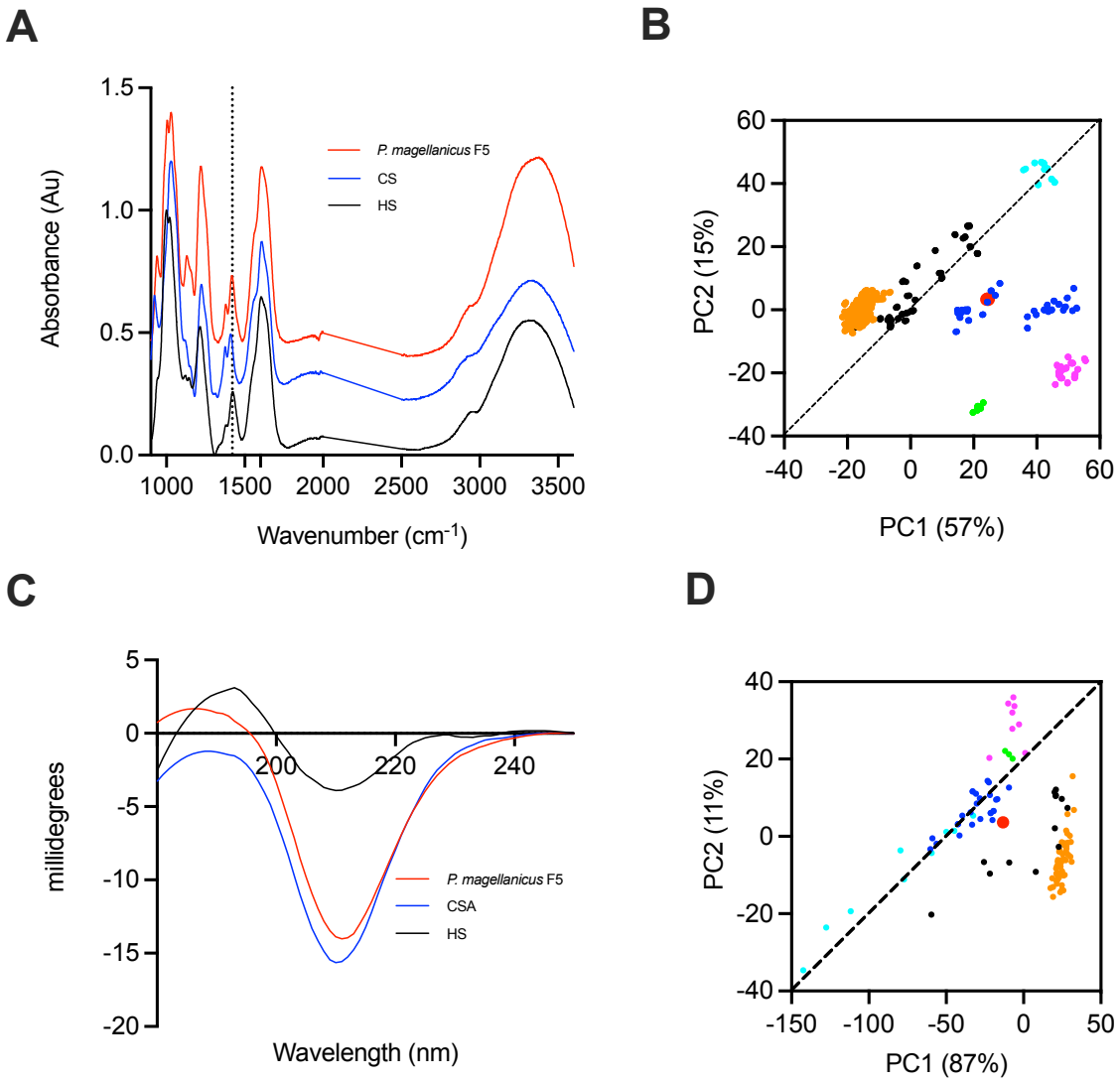

Figure 4. ATR-FTIR spectra of (A) *P. magellanicus F5* (red), CS (blue) and HS (black) (B) PCA of the ATR-FTIR spectra of *P. magellanicus* F5 (red) and a library of GAG standards; CS (blue), HS (black), HA (cyan), heparin (orange), DS (magenta) and OSCS (green). (C) CD spectra of *P. magellanicus* F5 (red), CS (blue) and HS (black). PCA of the CD spectra of *P. magellanicus* F5 (red) and a library of GAG standards; CS (blue), HS (black), HA (cyan), heparin (orange), DS (magenta) and OSCS (green).

In addition to ATR-FTIR, the circular dichroism (CD) spectra of GAGs can be utilised to approximate sample composition [33–35]. Differentiation of GAGs based upon their CD spectra is a result of the sensitivity of this technique to the conformation of the uronic acid residue, glycosidic linkage and the extent of polysaccharide sulphation. Again, post-acquisition PCA against a library of standards can be employed to further assist in the identification of GAGs present within a sample [35]. The CD spectrum of the *P. magellanicus* F5 extract exhibited a positive band at ~ 190 nm, which is indicative of a HS/heparin sample, and positive band at ~ 210 nm, which can be observed in all GAG standards, albeit to different extents [34]. When analysed by PCA, a comparison of

PC1 and PC2 (covering 98% of the total variance) separated the *P. magellanicus* F5 extract towards the region containing CS standards (Figure 4).

Since the band corresponding to HS/heparin within the *P. magellanicus* F5 extract, observed by agarose electrophoresis (Figure 3), was degraded by exhaustive digestion with *Pedobacter heparinus* lyases, the resulting products were subsequently analysed by strong anion-exchange high performance liquid chromatography (SAX-HPLC). The retention times of the *P. magellanicus* F5 disaccharide products were compared to those of the eight common HS/heparin Δ-disaccharide reference standards (Figure 5). Matched heparin and HS digest controls, with known compositions, were also employed to ensure that exhaustive enzymatic digestion of the *P. magellanicus* F5 extract had occurred (S1 and S2). A characteristic digestion profile was observed for porcine heparin with > 50% of the total disaccharide products being attributed to Δ-UA(2S)-GlcNS(6S) and ~ 20% to Δ-UA-GlcNS(6S) [36]. The disaccharide composition of the mammalian HS sample was also in accordance with the expected profile, with the most prevalent disaccharide being Δ-UA-GlcNAc at ~ 40%, which can be attributed to the NA domains of HS. Furthermore, the disaccharides Δ-UA-GlcNS (~ 20%), Δ-UA-GlcNAc(6S) (~ 15%), Δ-UA-GlcNS(6S) (20%) accounted for ~ 50% of the remainder of the disaccharides present within the HS sample, which is typical of a HS sample resulting from the NA/NS and NS-domains (Table 2).

Table 2. Disaccharide composition analysis of *P. magellanicus F5, HS and heparin.* N.D; not detected.

Δ-Disaccharide	*P. magellanicus* (%)	HS (%)	Heparin (%)
Δ-UA-GlcNAc	21	37	8
Δ-UA-GlcNS	1	18	3
Δ-UA-GlcNAc(6S)	64	14	6
Δ-UA(2S)-GlcNAc	2	N.D	3
Δ-UA-GlcNS(6S)	5	18	18
Δ-UA(2S)-GlcNS	<1	6	8
Δ-UA(2S)-GlcNAc(6S)	*N.D*	<1	2
Δ-UA(2S)-GlcNS(6S)	7	7	51

The disaccharide profile obtained from enzymatic digestion of the *P. magellanicus* F5 extract was in contrast to those observed for typical mammalian-derived HS and heparin samples. The unsulphated Δ-UA-GlcNAc disaccharide accounted for ~ 20% of the total detected disaccharides present within the *P. magellanicus* F5 extract, which is intermediary between the levels observed for heparin and HS samples (Table 2). The proportion of the trisulphated disaccharide, Δ-UA(2S)-GlcNS(6S) detected in the *P. magellanicus* F5 extract was, however, the same as that observed in the HS sample at ~ 10%. The most prevalent disaccharide detected within the *P. magellanicus* F5 extract was found to be Δ-UA-GlcNAc(6S) at 64%, this differs from both HS and heparin which both contain a low level of this mono-sulphated disaccharide. A low proportion of other mono-sulphated and di-sulphated disaccharides were also detected within the *P. magellanicus* F5 at > 10%, which again contrasts mammalian-derived HS and heparin. This suggest that the glucosaminoglycan component of the *P. magellanicus* F5 extract contains structural features that are distinct from mammalian samples, however, it should be noted

that some non-mammalian GAGs samples have been reported to resist comparable levels of digestion with heparin lyase enzymes obtained from *Pedobacter heparinus* [37].

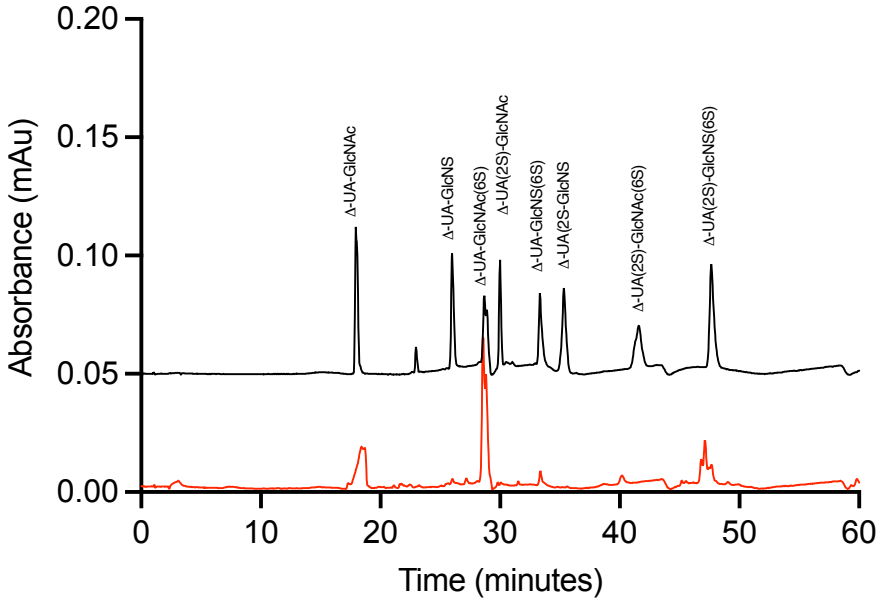

Figure 5. UV-SAX HPLC disaccharide composition analysis performed on the bacterial lyase digest of *P. magellanicus* F5 with reference to the eight common Hep/HS Δ- disaccharide standards. *P. magellanicus* F5 (red), Δ- disaccharide standards (black), 1; ΔUA-GlcNAc, 2; ΔUA-GlcNAc(6S), 3; ΔUA-GlcNS, 4; ΔUA-GlcNS(6S), 5; ΔUA(2S)-GlcNS, 6; ΔUA(2S)-GlcNS(6S), 7; ΔUA-(2S)-GlcNAc, 8; ΔUA(2S)-GlcNAc(6S). Elution was achieved using a linear gradient of 0 – 2 M NaCl (dashed line). Elution of Δ-disaccharides was monitored inline at 232 nm.

Proton and heteronuclear single-quantum correlation (HSQC) NMR spectroscopy were subsequently employed to further elucidate the composition of the GAGs present within the *P. magellanicus* F5 extract. Signals attributed to the N-Acetyl (NAc) of both Heparin/HS (~ 2.04 ppm) and CS (~ 2.02 ppm) could be observed within the *P. magellanicus* F5 extract (Figure 6A). Furthermore, signals corresponding to the anomeric carbon of glucosamine and carbon 2 of the N-sulphated glucosamine were also identified within the ^{1}H NMR of *P. magellanicus* F5 at ~ 5.4 ppm and ~ 3.25 ppm respectively, further indicating the presence of HS/heparin within the sample. The signal associated with anomeric carbon of galactosamine occurs in the region of 4.5 - 4.7 ppm; several resonances can be observed in this region within the ^{1}H NMR spectrum of the *P. magellanicus* F5 extract. As a result of the extensive overlapping resonances in the ^{1}H NMR spectra of GAGs, ^{1}H -^{13}C HSQC NMR was used for further assignment. Peak volume integration of the NAc signals corresponding to HS/heparin and CS/DS in the ^{1}H-^{13}C HSQC spectra of *P. magellanicus* F5 indicated that the sample contained a slighlty greater proportion of glucosaminoglycans than galactosaminoglycans (Figure 6B). Furthermore, resonances at 4.5 /103 ppm and 5.4/100 ppm are attributed to the anomeric carbons of galactosamine and glucosamine, respectively. Signals attributable to the anomeric carbon of IdoA, which occur downfield to signals corresponding to GlcA were not observed in the ^{1}H-^{13}C HSQC spectra of *P. magellanicus* F5 indicating that the GAGs lack significant levels of iduronic acid. The *P. magellanicus* F5 sample is therefore likely to be composed of HS-like glucosaminoglycans

and CS-like galactosaminoglycans. In addition, a minor signal attributed to carbon 2 of GlcNS was observed at ~ 3.2/58 ppm. Signals assigned to glucosamine 6S and 6OH were also observed at ~ 4.4/66 ppm and ~ 3.7/61 ppm, respectively. Peak volume integration of these signals indicates that the HS component of the *P. magellanicus* F5 sample is composed of ~ 60% glucosamine bearing sulphation at position 6. Minor signals attributed to 6-O-sulphated CS were also observed.

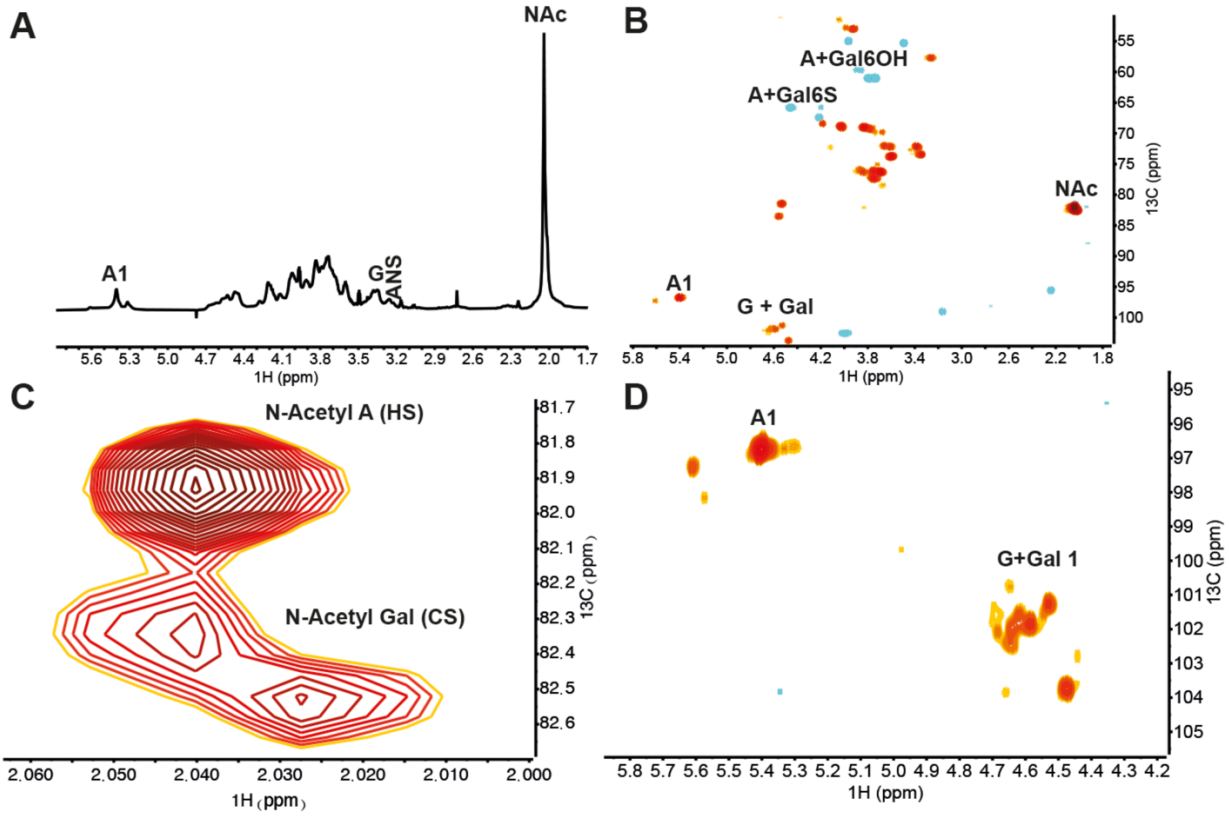

Figure 6 (A) ^{1}H and (B) ^{1}H-^{13}C HSQC NMR spectra of *P. magellanicus* F5; (C) expansion of the HSQC acetyl region; (D) expansion of the HSQC anomeric region. Major signals associated with CS and HS are indicated. Spectral integration was performed on the HSQC using labelled signals. Glucosamine, A; galactosamine, Gal; glucuronic acid, G.

3. Discussion

P. magellanicus tissue was utilised as source for the extraction of GAGs due to several bioactive compounds from this class of polysaccharides being previously identified within this species [38–40]. The GAG extract obtained from *P. magellanicus* following DEAE fractionation with 1M NaCl (F5) was observed to possess BACE-1 inhibitory activity at marginally reduced levels when compared to porcine heparin; IC_{50} = 4.8 µg. mL^{-1} and 2.5 µg. mL^{-1}, respectively. Furthermore, the *P. magellanicus* F5 extract was also observed to induce a reduction in the T_m of BACE-1 of Δ 8.8 °C, again this is approximately comparable to the ΔT_m of BACE-1 in the presence of porcine heparin (- 9.6 °C) when measured by DSF. Previously DSF, has been demonstrated to be a time and cost-efficient method for the initial evaluation of BACE-1 inhibitors. In contrast to small molecule inhibitors, GAGs induce a negative shift in the ΔT_m of BACE-1 when screened using this method [16,18,27,28,41]. Therefore, the initial assessment of the potential BACE-1 inhibitory activity of the *P. magellanicus* F5 extract using FRET and DSF measurements are promising and in line with previously identified GAG based inhibitors of BACE-1.

Despite the *P. magellanicus* F5 extract displaying marginally reduced potency for BACE-1 inhibition in comparison to porcine heparin, the former compound displayed a 25-fold reduction in activity in both the aPTT and PT assays, which measure the intrinsic and extrinsic coagulation pathways, respectively. As the potent anticoagulant activity of pharmaceutical heparin is unfavourable when considering the repurposing of this drug for alternative uses, for instance AD, the *P. magellanicus* F5 extract exhibits a greater therapeutic value in comparison to existing licenced heparin pharmaceuticals.

Structural analysis of the *P. magellanicus* F5 extract, revealed that the sample was composed of a mixture of HS and CS. Two bands were observed within the *P. magellanicus* F5 extract, which co-migrated with HS/heparin or CS/DS standards, when the sample was analysed by agarose-gel electrophoresis. The band which exhibited similar electrophoretic mobility to HS/heparin was more prominent and was also degraded by treatment with heparinase lyase enzymesfrom *Pedobactera heparinus.* Analysis of the FTIR-ATR and CD spectra of the *P. magellanicus* F5 extract also indicated that the sample was composed of a mixture of glycosaminoglycans and galactosaminoglycans, with these techniques suggest the mixture aligns towards CS, although the libraries which underpin such comparisons are composed exclusively of mammalian-derived GAGs and these would lack representation of modifications uncommon to those of mammalian provenance . Further structural analysis of the *P. magellanicus* F5 extract was performed using ^{1}H and ^{1}H-^{13}C HSQC NMR, the analysis of which supported the notion that the extract was composed of a mixture of both HS and CS. ^{1}H-^{13}C HSQC NMR also indicated that the HS component of *P. magellanicus* F5 contained only minor amounts of epimerised iduronic acid residues, with the primary uronate content being that of glucuronic acid. Furthermore, approximately 10% of the glucosamine residues were found to bear NS modifications, while ~ 60% were observed to possess sulphate at position 6. This was supported by disaccharide compositional analysis, which identified that the sample was composed of glucosamine residues with ~ 85% NAc, 70% 6S and 15% NS. Disaccharides possessing 2-sulphate modifications to the uronic acid residue were also observed when analysed by SAX HPLC, these were, however, not identified in the NMR spectra presumably due to the low prevalence of this modification. Previously 6S

modifications have been indicated to be important for BACE-1 inhibitory activity [15], while both epimerization and/or sulphation of the UA residue is largely unimportant [42]. The presence of a N-acetyl moety, as opposed to a N-sulphate modification, is known to reduce anticoagulant activity, whilst N-aceylation is preferential for BACE-1 inhibitory activity [15]. Therefore, the high prevalence of both 6-O-sulphated and N-acetylated glucosamine residues within the *P. magellanicus* F5 extract may account for the observed BACE-1 inhibitory activity of this sample. As the sample isolated from *P. magellanicus* F5 contains ~ 60% HS, further purification of this component may augment the BACE-1 inhibitory potential. That said, chondroitin sulphates have also been observed to possess BACE-1 inhibitory activity and the contribution of this component of the *P. magellanicus* F5 extract should not be excluded [17,18].

The isolation of GAGs, in particular HS with a high GlNAc(6S) content, from *P. magellanicus* F5 is therefore significant for the exploration of inhibitors based upon this class of polysaccharide. HS bearing GlcNAc(6S) is typically a minor component of mammalian HS or heparin samples (Table 2) as a result of O-sulfation modifications during biosynthesis principally occurring subsequent to N-sulphation [43]. Glycosaminoglycans isolated from aquatic species are known to possess modifications that are considered rare in comparison to their mammalian counterparts [3,16–26]. Aquatic species offer additional sequence space, which may be beneficial for alternative applications as demonstrated here for BACE-1 inhibition. Furthermore, GAGs isolated from aquatic species offer the additional advantage that they are likely to be free from harbouring mammalian pathogens, such as bovine spongiform encephalopathies, which have previously led to the removal of bovine heparin sources from the market. Furthermore, many aquatic organisms such as *P. magellanicus* can be cultivated via aquaculture, making them a viable, economical and sustainable alternative to mammalian sources of GAGs. Further investigations should be conducted to evaluate whether GAGs possessing favourable bioactivities can be isolated from by-products of *P. magellanicus* production for the food industry, for example the viscera. Further research and knowledge of the biologically active sequences present within the *P. magellanicus* extract could also unlock potential for both chemoenzymatic and chemical synthesis routes, ultimately providing a pathway to larger scale saccharide production. Furthermore, it can be envisaged that the highly expanded GAG sequence space that aquatic organisms possess could inform and augment future synthesis routes, yielding novel, next-generation GAG-based therapeutics.

4. Methods

4.1 Isolation of glycosaminoglycans from Placopecten magellanicus

Prior to extraction, approximately 3 kg of *Placopecten magellanicus* tissue (Wm. Morrisons, UK) was blended in an excess of acetone (VWR, UK), incubated for 24 hours (r.t). and centrifuged at 5,670 g for 10 minutes. The liquid layer was discarded, and the remaining tissue incubated overnight (r.t.) to allow the evaporation of residual acetone. The defatted tissue was digested with Alcalase (17 $U.kg^{-1}$; Novozymes, Bagsvaerd, Denmark) for 24 hours at 60 °*C* in PBS (supplemented to 1M NaCl, at pH 8.0). Particulate matter was removed and discarded (centrifugation at 5,670 g) and the resultant solution incubated with ion-exchange resin (Amberlite IRA-900 ion, OH- from; Sigma-Aldrich, Dorset UK) for 24 hours at r.t. with gentle agitation. The ion-exchange resin was recovered and washed (10 volumes of dH_2O followed by 1 M NaCl) prior to elution in 3 M NaCl (24 hours, under agitation). A crude GAG extract was obtained following precipitation of the aforementioned eluent in methanol (1:1 v/v) for 48 hours at 4°*C* (VWR, Lutterworth, UK). The resulting precipitate was recovered by centrifugation at 15,400 g (4°*C)* for 1 hour, desalted via dialysis for 48 hours against dH_2O (3.5 kDa MWCO; Biodesign, NY, USA), and lyophilised. The crude GAG extract was further fractionated using weak anion exchange chromatography (DEAE-Sephacel, 10 mm I.D. x 10 cm; GE Healthcare, Buckinghamshire, UK). Fractions were eluted using a step-wise gradient of NaCl at a flow rate of 1 $mL.min^{-1}$, with in-line monitoring at 232 nm and 210 nm (Cecil Instruments, Cambridge, UK). Six fractions (F1-6), corresponding to 0, 0.25, 0.5, 0.8, 1 and 2M NaCl respectively, were collected, dialysed against dH_2O for 48 hours and lyophilised prior to storage (4°*C*).

4.2 Agarose-based Gel Electrophoresis

Electrophoretic separation of GAGs (5 µg) was achieved using a 0.55% (*w/v*) agarose gel (80 x 80 x 1.5 mm) in 50 mM 1,3-diaminopropane-acetate (pH 9.0; VWR, Altrincham, UK) run in the same buffer at 105 V for 30 mins. Post migration, precipitation of the separated GAG bands within the gel was achieved through the immersion of the gel in cetyltrimethylammonium bromide solution (0.1% w/v) for 4 hours. The gel was dried overnight before staining with Toluidine Blue (0.1% w/v in acetic acid:ethanol:H_2O (0.1:5:5 v/v)) for 1 hour. The gel was destained in acetic acid:ethanol:H_2O (0.1:5:5 v/v) prior to image acquisition and processing using GIMP software (v2.8, Berkeley, CA, USA) and Image J (v1.51 (100), Madison, QI, USA), respectively.

4.3 Fourier Transform Infrared Spectroscopy (Attenuated Total Reflectance)

Fourier Transform Infrared Spectra (Bruker Alpha 1 instrument) were recorded using Attenuated Total Reflectance of the freeze-dried sample (10 mg) with 5 repeats of an average of 32 scans permed at a spectral resolution of 2 cm^{-1} (400 – 4000 cm^{-1}). Spectral acquisition, background correction and data analysis were

performed using an Asus Vivibook Pro (M580VD-EB76, Taiwan) using Opus (v8.1, Bruker, UK) and R Studio (v1.1.463) software. Spectra were smoothed using a Savitzky-Golay filter (2nd degree polynomial, 21 neighbours) prior to baseline correction (7th-order polynomial; normalisation between 0–1). Spectral regions between 2000 -2500 cm^{-1}, above 3600 cm^{-1} and below 700 cm^{-1}, were excluded from post-acquisition PCA to restrict the effects of environmental variations (CO_2 and H_2O regions). Second derivative curves (Savitzky–Golay algorithm, 2nd order polynomial with 41 neighbours) were subsequently obtained and PCA was performed on the normalised, corrected matrices of intensities, deploying singular value decomposition within R studio (mean-centered, base prcomp function).

4.4 High Performance Liquid Chromatography HS/heparin disaccharide compositional analysis.

Both P. magellanicus F5 ,heparin (porcine mucosal) and HS (bovine) control samples (50 µg each) were exhaustively digested by *Pedobacter heparinus* lyase enzymes (Iduron, UK) in 25 mM sodium acetate, 5 mM calcium acetate, pH 7.0, added sequentially at 4 hours intervals (heparinase I, III and II; 2.5 mIU.mg^{-1}; 37 °C) before overnight incubation at 37 °C. A pre-equilibrated (HPLC-grade H_2O) ProPac PA-1 analytical column (4 × 250 mm, Dionex, UK) was employed for the separation of the resultant Δ-disaccharides using a 1-hour linear gradient between 0 - 2 M NaCl (HPLC grade; VWR, UK) with in-line detection at 232 nm. The identification of eluted standards was carried out through correlation with a reference chromatogram containing the 8 common Δ-disaccharide reference standards (Iduron, UK) for heparin according to [36].

4.5 Nuclear Magnetic Resonance

P. magellanicus F5 was freeze-dried and resuspended in D_2O (600 µL; VWR, UK) thrice prior to data acquisition. NMR experiments were carried out using an Avance Neo 800 MHz spectrometer with a 5 mm TXI Probe (Bruker, UK) at 298 K. Both 1-D (^{1}H) spectra and 2D ^{1}H–^{13}C Heteronuclear Single-Quantum Correlation (HSQC) spectra were collected employing standard pulse sequences. Spectra were processed and plotted using TopSpin (Bruker, UK).

4.6 FRET-based BACE-1 activity assays

Both P. magellanicus F5 and heparin were assayed for inhibitory activity against human BACE-1 (tag free; ACRO Biosystems, USA), using a fluorescence resonance energy transfer (FRET) assay (λ_{ex} 320 nm, λ_{em} 405 nm). hBACE1 (312.5 ng) and *Placopecten magellanicus* F5 or heparin were incubated for 10 mins (37 °C) in 50 mM sodium acetate (pH 4.0) prior to the addition of peptidic FRET substrate (MCA-SEVNLDAEFRK(DNP)RR-NH2; Biomatik, Canada; 6.25 µM), which was also pre-incubated at 37 °C for 10 min (final volume, 50 µL). Emission was

monitored over a 90 mins period using a Tecan Infinite® M200 Pro plate reader with i-control™ software (Tecan, Switzerland). Δ RFU.min^{-1} was calculated through the linear range of the control containing no inhibitor, with normalised percentage inhibition calculated (% ± SD, n = 3) via the mean of the substrate only and no inhibitor controls. A four-parameter logistics model was subsequently fitted using Prism 7 (GraphPad Software, San Diego, CA, USA). For assays performed with *Placopecten magellanicus* F5 treated with either chondroitin ABC lyase (Sigma-Aldrich, UK) or heparinase I & III (Iduron, UK), *Placopecten magellanicus* F5 extract was digested overnight at 37 °C (2.5 mIU.mg-1) prior to the determination of BACE-1 inhibitory activity.

4.7 Activated Partial Thromboplastin Time

Normal human plasma (pooled, with citrate; Technoclone, UK), Pathromtin SL reagent (Siemens, Germany) and test sample (*P. magellanicus* F5 or heparin control; 2:2:1 v/v, 150 uL) were incubated for 2 minutes at 37 °C prior to the addition of 50 mM $CaCl_2$ (50 uL; VWR, UK). The time taken for clot formation to occur was measured using a Thrombotrak Solo coagulometer (Axis-Shield, UK) and an upper limit of 120 seconds (representing 100% clotting inhibition) was imposed. Water (0% inhibition of clotting, representing a normal aPTT clotting time, of circa. 37 – 40 s) and porcine mucosal heparin (193 IU.mg^{-1}; Celsus, OH, USA) were used as controls. EC_{50} values were determined through the fitting of a sigmoidal dose response curve (GraphPad Prism 7, CA, USA).

4.8 Prothrombin Time

Normal human plasma (pooled, with citrate; Technoclone, UK; 50 uL) and test sample (*P. magellanicus* F5 or heparin control; 50 uL) were incubated for 2 minutes at 37 °C prior to the addition of Thromborel S reagent (Siemens, Germany; 50 uL). The time taken for clot formation to occur was measured using a Thrombotrak Solo coagulometer (Axis-Shield, UK) and an upper limit of 120 seconds (representing 100% clotting inhibition) was imposed. Water (0% clot inhibition, representing a normal PT clotting time of circa. 13 – 14 s) and porcine heparin (193 IU mg^{-1}; Celsus, USA) were used as controls. EC_{50} values were determined through the fitting of a sigmoidal dose response curve (GraphPad Prism 7, CA, USA).

4.9 Differential Scanning fluorimetry

Differential scanning fluorimetry experiments were performed using a StepOne plus qPCR machine (AB Biosystems, UK; TAMRA filter) on human BACE-1 (1 µg) in sodium acetate buffer (50 mM, pH4.0) with or without f *P. magellanicus* F5 [41,42]. 20x Sypro Orange was also included as a reporter dye in a final well volume of 40 µl (96-well qPCR plates; VWR, UK). Melt curves were generated via an initial incubation of 2 mins at 20 °C, followed by 0.5 °C increments every 30 s, up to a T_{max} of 90 °C. Data analysis was carried out using Prism 7

543 software (GraphPad, San Diego, CA, USA), plotting the Savitzky-Golay smoothed first-derivative (19 neighbours;
544 2nd-order polynomial). T_m values were obtained from first derivative peaks.
545
546
547 *4.10 Circular dichroism*
548
549 The circular dichroism spectra of *P. magellanicus* F5 and other relevant GAGs standards (10 mg.ml^{-1}) in HPLC-
550 grade H_2O (VWR, UK) were recorded on a J-1500 Jasco CD spectrometer controlled via Spectral Manager II
551 software. Instrument calibration was performed prior to use, using (+)-10-camphorsulfonic acid (1 mg.mL^{-1}) as
552 a spectral reference. A scan speed of 100 nm.min^{-1} with 1 nm resolution (180–260 nm) was utilised in concert
553 with a 0.2 mm pathlength, quartz cuvette (Hellma, USA). Spectra obtained were the mean of five independent
554 scans and data was further processed using GraphPad Prism 7 (smoothed to 9 neighbours, 2nd-order
555 polynomial). Post-acquisition, PCA was performed in R studio, utilising the singular value decomposition (SVN),
556 base prcomp function with mean centering of the matrices (v1.1.463, R studio Inc. Boston, MA, USA).
557
558
559 **Author Contributions:** M.A.S., C.J.M.-W. and L.C.C. designed and conceived the project. C.J.M.-W., A.J.D. and
560 M.A.S. performed FTIR spectroscopy and carried out principal component analysis on associated data sets.
561 C.J.M.-W., M.A.S., M.A.L. and M.G. performed and analysed the NMR data. C.J.M.-W. performed all other
562 experimentation whilst M.A.S, A.J.D., L.CC.., P.P., S.E.G., and D.G.F. provided assistance. C.J.M.-W. and M.A.S.
563 wrote the manuscript and all authors contributed to the editing and approval of the final version of the
564 manuscript.
565
566 **Funding:** The authors would like to thank the Engineering and Physical Sciences Research Council, UK; the
567 Biotechnology and Biological Sciences Research Council, UK; the Medical Research Council, UK; the Royal
568 Society, UK; Intellihep Limited, UK; The Royal Society, UK; MI Engineering Limited, UK; Financiadora de Estudos
569 e Projetos (FINEP), Brazil and Keele University, UK for the financial support that has been provided.
570
571 **Acknowledgements:** The authors would like to thank Dr. Matthew Cliff for NMR technical assistance.
572
573 **Conflicts of Interest:** The funders had no role in the study design, data collection and interpretation, or the
574 decision to submit the work for publication.
575
576
577
578
579
580
581
582

References

1. Couchman JR, Pataki CA. An Introduction to Proteoglycans and Their Localization. J Histochem Cytochem. 2012;60(12):885–97.
2. Hook M, Kjellen L, Johansson S, Robinson J. Cell-Surface Glycosaminoglycans. Annu Rev Biochem. 1984;53:847–69.
3. Mycroft-West CJ, Yates EA, Skidmore MA. Marine glycosaminoglycan-like carbohydrates as potential drug candidates for infectious disease. Biochem Soc Trans. 2018;46(4).
4. Prydz K. Determinants of glycosaminoglycan (GAG) structure. Biomolecules. 2015;5(3):2003–22.
5. Snow AD, Cummings JA, Lake T. The Unifying Hypothesis of Alzheimer's Disease: Heparan Sulfate Proteoglycans/Glycosaminoglycans Are Key as First Hypothesized Over 30 Years Ago. Vol. 13, Frontiers in Aging Neuroscience. Frontiers Media S.A.; 2021.
6. Scholefield Z, Yates EA, Wayne G, Amour A, McDowell W, Turnbull JE. Heparan sulfate regulates amyloid precursor protein processing by BACE1, the Alzheimer's beta-secretase. J Cell Biol. 2003 Oct 13;163(1):97–107.
7. Cai H, Wang Y, McCarthy D, Wen H, Borchelt DR, Price DL, et al. BACE1 is the major β-secretase for generation of Aβ peptides by neurons. Nat Neurosci. 2001 Mar 1;4(3):233–4.
8. Querfurth HW, LaFerla FM. Alzheimer's Disease. N Engl J Med. 2010 Jan 28;362(4):329–44.
9. Vaz M, Silvestre S. Alzheimer's disease: Recent treatment strategies. Eur J Pharmacol. 2020;887(May):173554.
10. Vassar R. BACE1 inhibition as a therapeutic strategy for Alzheimer's disease. J Sport Heal Sci. 2016 Dec;5(4):388–90.
11. Leveugle B, Ding W, Laurence F, Dehouck MP, Scanameo A, Cecchelli R, et al. Heparin oligosaccharides that pass the blood-brain barrier inhibit beta-amyloid precursor protein secretion and heparin binding to beta-amyloid peptide. J Neurochem. 1998 Feb;70(2):736–44.
12. Bergamaschini L, Rossi E, Vergani C, De Simoni MG. Alzheimer's disease: Another target for heparin therapy. ScientificWorldJournal. 2009;9:891–908.
13. Timmer NM, van Dijk L, der Zee CEEM van, Kiliaan A, de Waal RM., Verbeek MM. Enoxaparin treatment administered at both early and late stages of amyloid β deposition improves cognition of APPswe/PS1dE9 mice with differential effects on brain Aβ levels. Neurobiol Dis. 2010 Oct;40(1):340–7.
14. Wu L, Jiang W, Zhao N, Wang F. Heparan sulfate from porcine mucosa promotes amyloid-beta clearance in APP/PS1 mice and alleviates Alzheimer's pathology. Carbohydr Polym. 2022 Jun 1;285.
15. Susannah J. Patey, Elizabeth A. Edwards, Edwin A. Yates † and, Jeremy E. Turnbull* †. Heparin Derivatives as Inhibitors of BACE-1, the Alzheimer's β-Secretase, with Reduced Activity against Factor Xa and Other Proteases. 2006;
16. Mycroft-West CJ, Cooper LC, Devlin AJ, Procter P, Guimond SE, Guerrini M, et al. A Glycosaminoglycan Extract from Portunus pelagicus Inhibits BACE1, the β Secretase Implicated in Alzheimer's Disease. Mar Drugs. 2019;17(5):293.
17. Mycroft-West CJ, Devlin AJ, Cooper LC, Procter P, Miller GJ, Fernig DG, et al. Inhibition of BACE1, the β-secretase implicated in Alzheimer's disease, by a chondroitin sulfate extract from Sardina pilchardus. Neural Regen Res. 2020;15(8).
18. Mycroft-West CJ, Devlin AJ, Cooper LC, Guimond SE, Procter P, Guerrini M, et al. Glycosaminoglycans from Litopenaeus vannamei Inhibit the Alzheimer's Disease β Secretase, BACE1. Mar Drugs. 2021 Apr 3;19(4).
19. Valcarcel J, Nova-Carballal R, Perez-Martin IR, Reis LR, Vazeuez AJ. Glycosaminoglycans from marine sources as therapeutic agents. Biotechnol Adv. 2017;1(35):711–25.
20. Bergefall K, Trybala E, Johansson M, Uyama T, Yamada S, Kitagawa H, et al. Chondroitin sulfate characterized by the E-disaccharide unit is a poten inhibtor of herpes simplex virus infectivity and provides the virus binding sites on gro2C cells. J Biolochical Chem. 2005;280(37):32193–9.
21. Wu M, Huang R, Wen D, Gao N, He J, Li Z, et al. Structure and effect of sulfated fucose branches on anticoagulant activity of the fucosylated chondroitin sulfate from sea cucumber Thelenata ananas. 2012;87:862–8.
22. Brito AS, Arimatéia DS, Souza LR, Lima MA, Santos VO, Medeiros VP, et al. Anti-inflammatory properties of a heparin-like glycosaminoglycan with reduced anti-coagulant activity isolated from a marine shrimp. Bioorg Med Chem. 2008;16(21):9588–95.
23. Chavante SF, Santos EA, Oliveira FW, Guerrini M, Torri G, Casu B, et al. A novel heparan sulphate with high degree of N -sulphation and high heparin cofactor-II activity from the brine shrimp Artemia

franciscana. 2000;27:49–57.
24. Palhares LCGF, Brito AS, de Lima MA, Nader HB, London JA, Barsukov IL, et al. A Further Unique Chondroitin Sulfate from the shrimp Litopenaeus vannamei with Antithrombin Activity that Modulates Acute Inflammation. Carbohydr Polym. 2019;222(April):115031.
25. Chavante SF, Brito AS, Lima M, Yates E, Nader H, Guerrini M, et al. A heparin-like glycosaminoglycan from shrimp containing high levels of 3-O-sulfated D -glucosamine groups in an unusual trisaccharide sequence. Carbohydr Res. 2014;390:59–66.
26. Cavalcante RS, Brito AS, Palhares LCGF, Lima MA. 2 , 3-Di- O -sulfo glucuronic acid : An unmodi fi ed and unusual residue in a highly sulfated chondroitin sulfate from Litopenaeus vannamei. Carbohydr Polym. 2018;183(December 2017):192–200.
27. Lo M-C, Aulabaugh A, Jin G, Cowling R, Bard J, Malamas M, et al. Evaluation of fluorescence-based thermal shift assays for hit identification in drug discovery. Anal Biochem. 2004 Sep 1;332(1):153–9.
28. Chambers M, Delport A, Hewer R. The use of the cellular thermal shift assay for the detection of intracellular beta-site amyloid precursor protein cleaving enzyme-1 ligand binding. Mol Biol Rep. 2021 Mar 1;48(3):2957–62.
29. Devlin A, Mycroft-west CJ, Guerrini M, Yates EA. Analysis of solid-state heparin samples by ATR-FTIR spectroscopy . 2019;
30. Grant D, Long WF, Moffat CF, Williamson FB. Infrared spectroscopy of chemically modified heparins. Biochem J. 1989;261(3):1035–8.
31. Vasko PD, Blackwell J, Koenig JL. Infrared and raman spectroscopy of carbohydrates. Part I: Identification of OH and CH-related vibrational modes for D-glucose, maltose, cellobiose, and dextran by deuterium-substitution methods. Carbohydr Res. 1971 Oct 1;19(3):297–310.
32. Myron P, Siddiquee S, Azad S Al. Partial structural studies of fucosylated chondroitin sulfate (FuCS) using attenuated total reflection fourier transform infrared spectroscopy (ATR-FTIR) and chemometrics. Vol. 89, Vibrational Spectroscopy. Elsevier B.V.; 2017. 26–36 p.
33. Rudd T, Fernig DG, Turnbull JE, Brown A, Guimond S, Skidmore M, et al. Site-specific interactions of copper(II) ions with heparin revealed with complementary (SRCD, NMR, FTIR and EPR) spectroscopic techniques. Carbohydr Res. 2008;343(12):2184–93.
34. Rudd T, Yates E, Hricovini M. Spectroscopic and Theoretical Approaches for the Determination of Heparin Saccharide Structure and the Study of Protein-Glycosaminoglycan Complexes in Solution. Curr Med Chem. 2009;16(35):4750–66.
35. Rudd T, Skidmore M, Guimond S, Holman J, Turnbull J. The potential for circular dichroism as an additional facile and sensitive method of monitoring low-molecular-weight heparins and heparinoids. Thromb Haemost. 2009;102.
36. Skidmore MA, Guimond SE, Turnbull JE, Dumax-Vorzet AF, Yates EA, Atrih A. High sensitivity separation and detection of heparan sulfate disaccharides. J Chromatogr A. 2006;1135(1):52–6.
37. Dietrich CP, Tersariol IL, Toma L, Moraes CT, Porcionatto MA, Oliveira FW, et al. Structure of heparan sulfate: identification of variable and constant oligosaccharide domains in eight heparan sulfates of different origins. Cell Mol Biol (Noisy-le-grand). 1998 May;44(3):417–29.
38. Saravanan R, Shanmugam A. Isolation and Characterization of Low Molecular Weight Glycosaminoglycans from Marine Mollusc Amussium pleuronectus (Linne) using Chromatography. 2010;791–9.
39. Gomes. Unique Extracellular Matrix Heparan Sulfate from the Bivalve Nodipecten nodosus (Linnaeus , 1758) Safely Inhibits Arterial Thrombosis after Photochemically Induced Endothelial Lesion *. 2010;285(10):7312–23.
40. Valcarcel J, Novoa-Carballal R, Pérez-Martín RI, Reis RL, Vázquez JA. Glycosaminoglycans from marine sources as therapeutic agents. Biotechnol Adv. 2017;35(6):711–25.
41. Mycroft-West CJ, Devlin AJ, Cooper LC, Procter P, Miller GJ, Fernig DG, et al. Inhibition of BACE1, the β-secretase implicated in Alzheimer's disease, by a chondroitin sulfate extract from Sardina pilchardus. Neural Regen Res. 2020;15(8):1546–53.
42. Schwörer R, Zubkova O V., Turnbull JE, Tyler PC. Synthesis of a targeted library of heparan sulfate hexa- to dodecasaccharides as inhibitors of β-secretase: Potential therapeutics for Alzheimer's disease. Chem - A Eur J. 2013;19(21):6817–23.
43. Kreuger J, Kjellén L. Heparan Sulfate Biosynthesis: Regulation and Variability. J Histochem Cytochem. 2012 Oct 4;60(12):898–907.
44. Uniewicz K a, Ori A, Xu R, Ahmed Y, Fernig DG, Yates E a. Differential Scanning Fluorimetry measurement of protein stability changes upon binding to glycosaminoglycans : a rapid screening test

for binding specificity Figure S-1 Sequence data for tested FGF-s Figure S-2 Sulfation pattern of the major repeating di. 2010;82(9):1–3.

45. Niesen FH, Berglund H, Vedadi M. The use of differential scanning fluorimetry to detect ligand interactions that promote protein stability. Nat Protoc. 2007 Sep;2(9):2212–21.

Supplementary

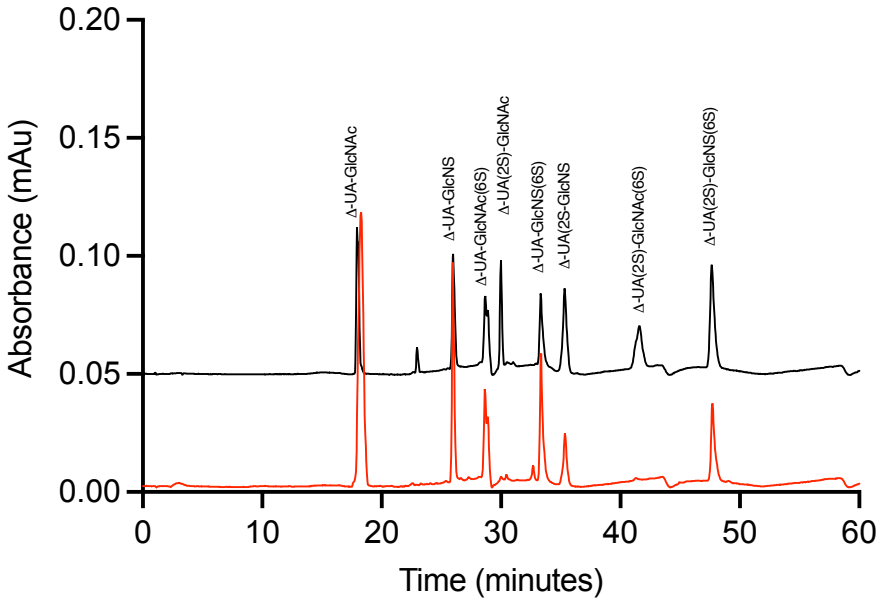

S1. UV-SAX HPLC disaccharide composition analysis performed on the bacterial lyase digest of HS with reference to the eight common Hep/HS Δ- disaccharide standards. HS (black), Δ- disaccharide standards (dashed line), 1; ΔUA-GlcNAc, 2; ΔUA-GlcNAc(6S), 3; ΔUA-GlcNS, 4; ΔUA-GlcNS(6S), 5; ΔUA(2S)-GlcNS, 6; ΔUA(2S)-GlcNS(6S), 7; ΔUA-(2S)-GlcNAc, 8; ΔUA(2S)-GlcNAc(6S). Elution was achieved using a linear gradient of 0 – 2 M NaCl (dashed line). Elution of Δ-disaccharides was monitored inline at 232 nm.

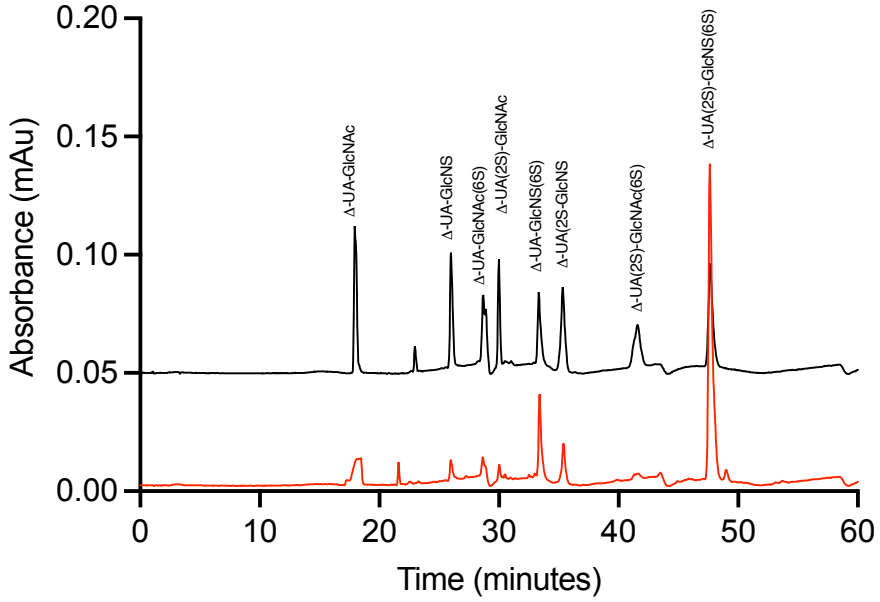

S2. UV-SAX HPLC disaccharide composition analysis performed on the bacterial lyase digest of heparin with reference to the eight common Hep/HS Δ- disaccharide standards. Heparin (black), Δ- disaccharide standards (dashed line), 1; ΔUA-GlcNAc, 2; ΔUA-GlcNAc(6S), 3; ΔUA-GlcNS, 4; ΔUA-GlcNS(6S), 5; ΔUA(2S)-GlcNS, 6; ΔUA(2S)-GlcNS(6S), 7; ΔUA-(2S)-GlcNAc, 8; ΔUA(2S)-GlcNAc(6S). Elution was achieved using a linear gradient of 0 – 2 M NaCl (dashed line). Elution of Δ-disaccharides was monitored inline at 232 nm.

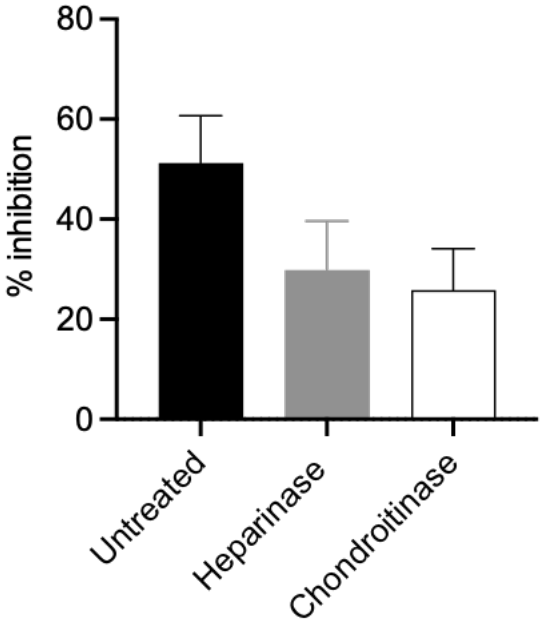

S3. BACE-1 inhibitory activity of *P. magellanicus* F5 (6 μg.mL^{-1}) untreated (51% BACE-1 inhibition, SD= 9; n= 6) or digested with chondroitinase ABC (26% BACE-1 inhibition, SD= 9; n= 6) or heparinase I and III (30% BACE-1 inhibition, SD= 9; n= 6). BACE-1 inhibitory activity determined by a quenched fluorogenic FRET peptide assay.